SUPPORTING INFORMATION

Discovery of a Pair of Diastereomers as Potent HDACs Inhibitors: Determination of Absolute Configuration, Biological Activity Comparison and Computational Study.

Yingjie Zhang,[a] *Elizabeth S. Inks,*[b] *Mengyuan Zhu,*[c] *C. James Chou,*[b] *Hao Fang,*[a] *Minyong Li,*[c] *Yuemao Shen,*[c] *Fan Yi,*[d] *and Wenfang Xu**[a]

[a] Department of Medicinal Chemistry, School of Pharmaceutical Sciences, Shandong University, Ji'nan, Shandong, 250012, P. R. China.

[b] Department of Drug Discovery and Biomedical Sciences, South Carolina College of Pharmacy, Medical University of South Carolina, Charleston, South Carolina, 29425, United States.

[c] Key Laboratory of Chemical Biology (Ministry of Education), School of Pharmaceutical Sciences, Shandong University, Ji'nan, Shandong, 250012, P. R. China.

[d] Department of Pharmacology, School of Medicine, Shandong University, Ji'nan, Shandong, 250012, P. R. China.

Contents

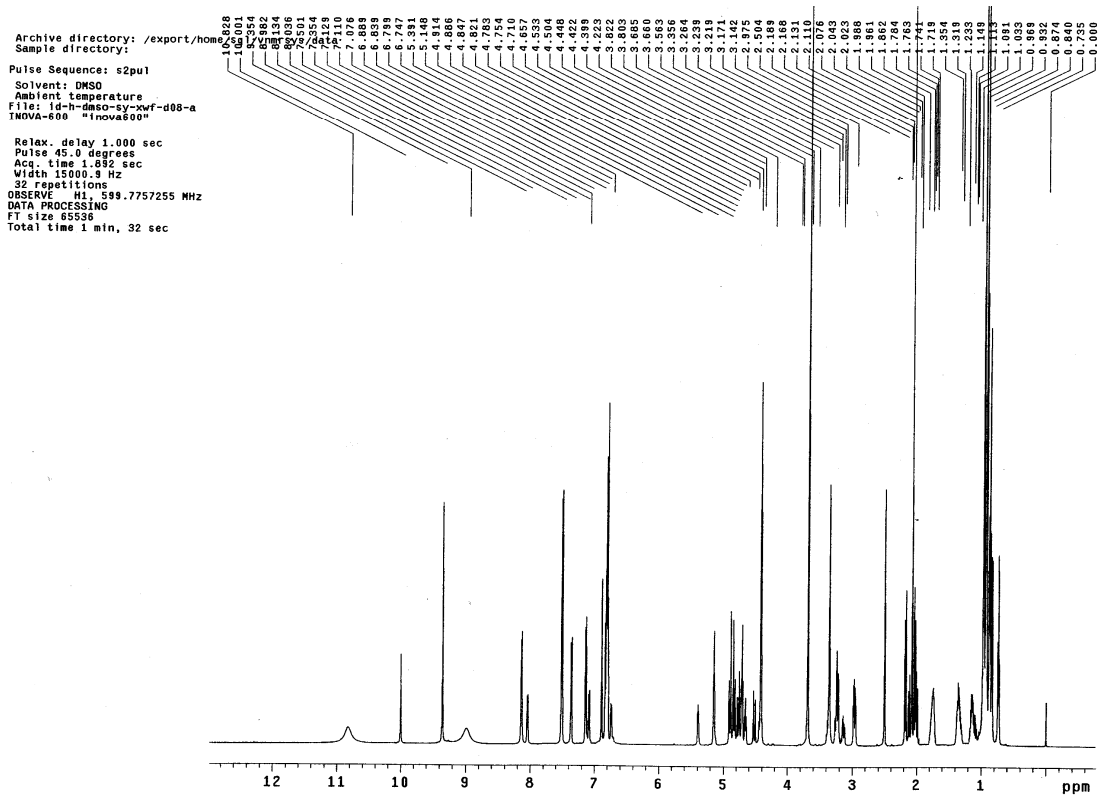

Fig. S1. ^{1}H NMR of ZYJ-34c

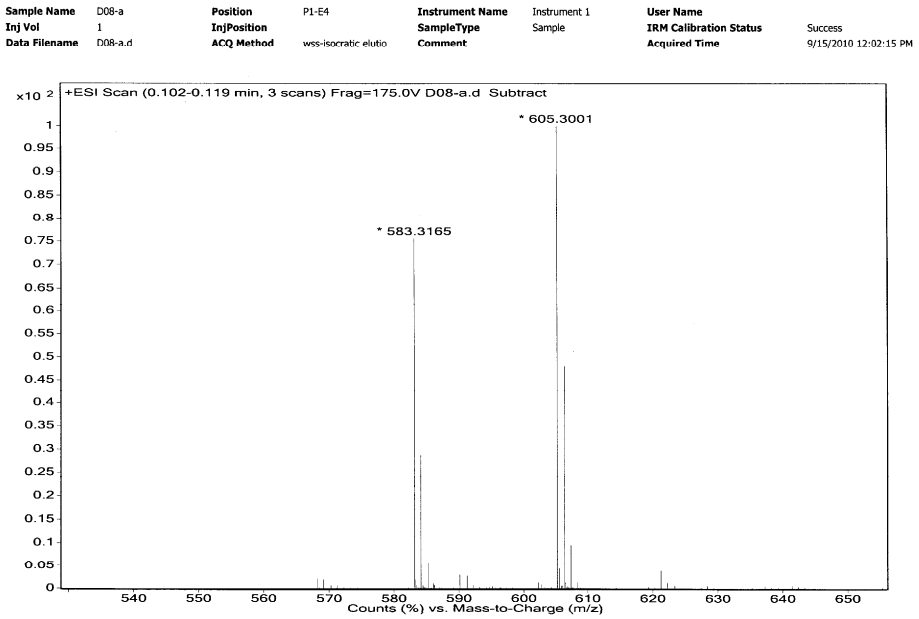

Fig. S2. HRMS of ZYJ-34c

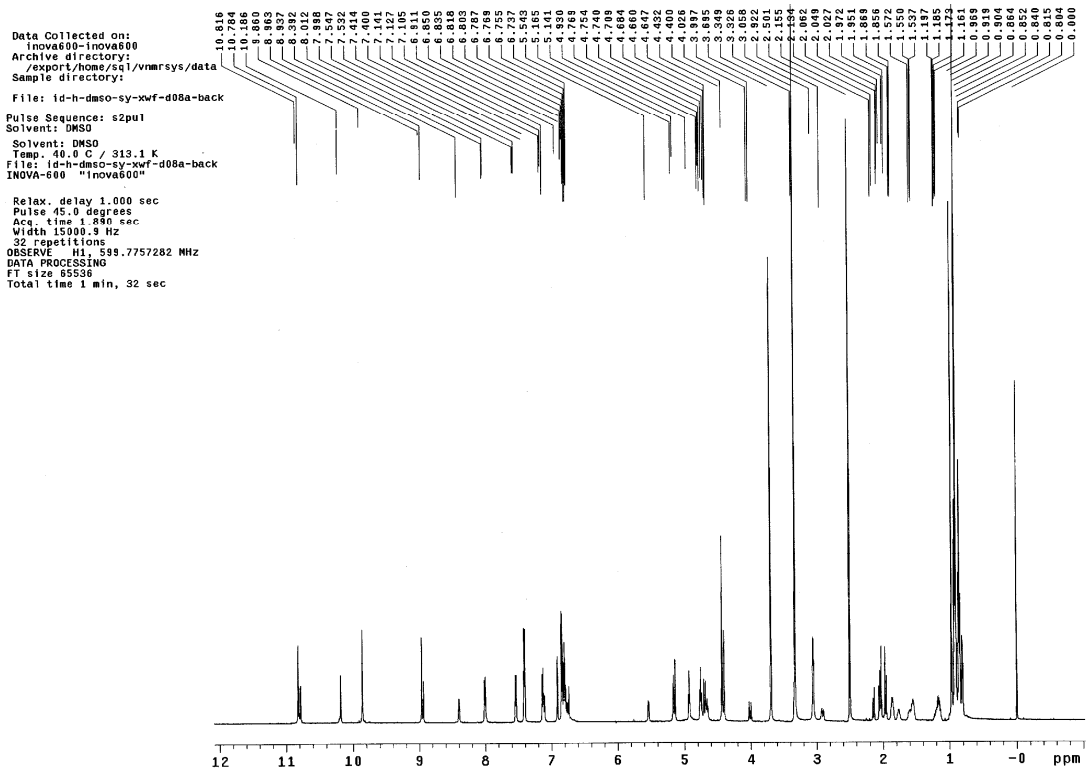

Fig. S3. ^{1}H NMR of ZYJ-34c epimer

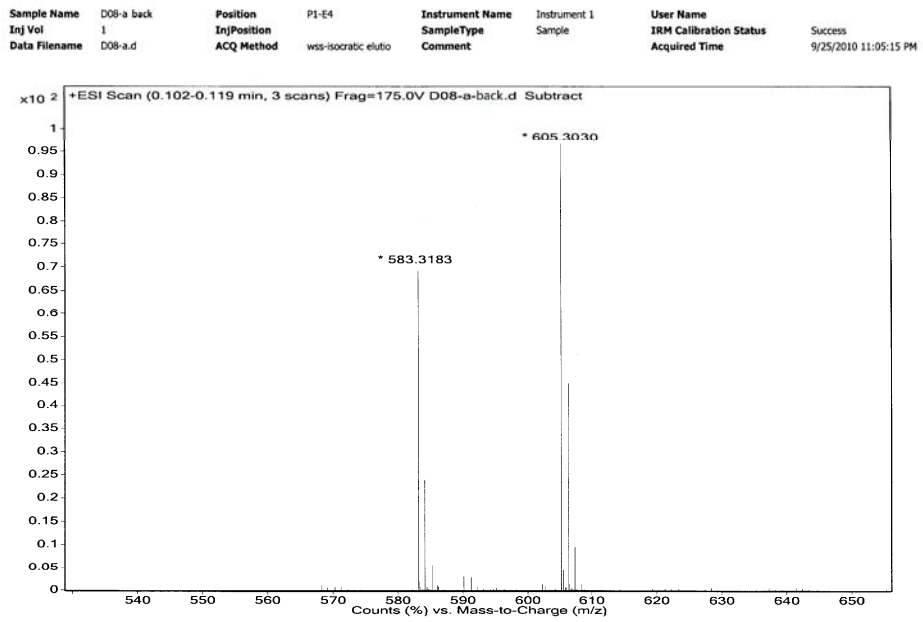

Fig. S4. HRMS of ZYJ-34c epimer

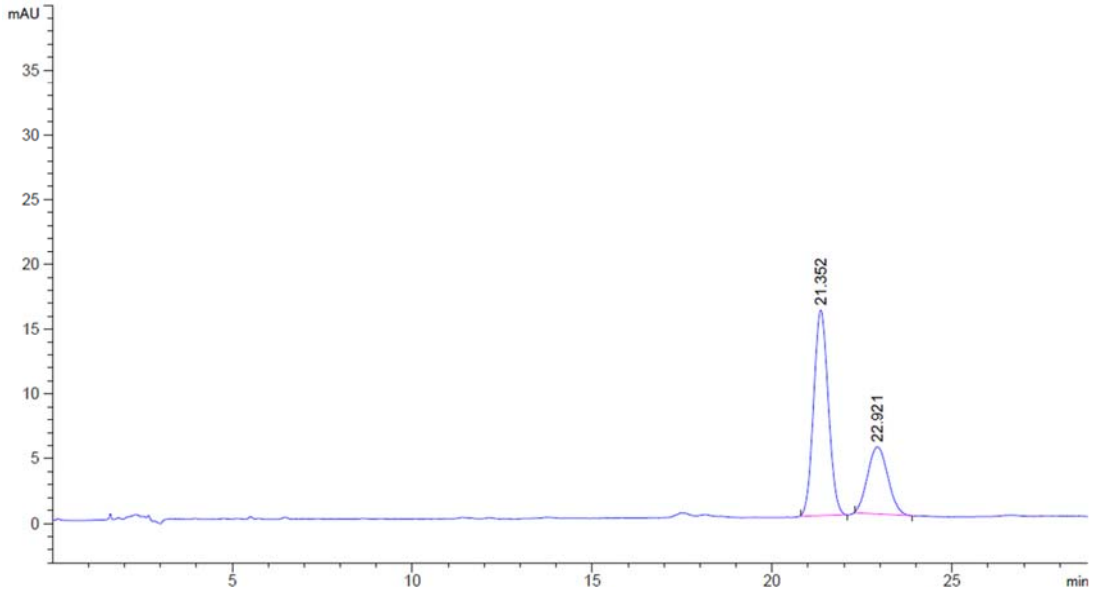

Fig. S5. HPLC chromatogram of racemic mixture of intermediate **10** synthesized in Scheme 1

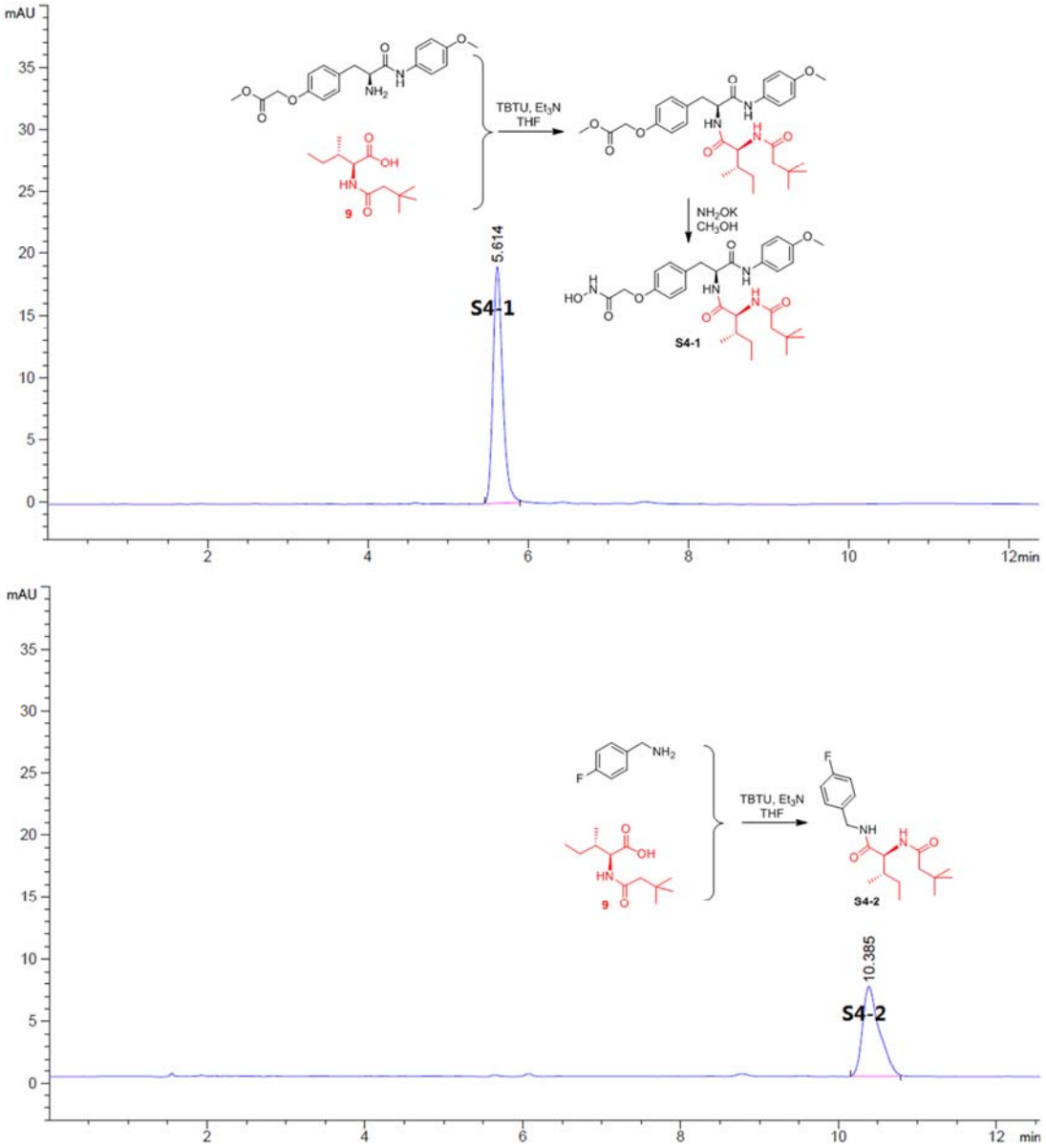

Fig. S6. Synthesis routes and HPLC chromatograms of compounds **S4-1** and **S4-2**

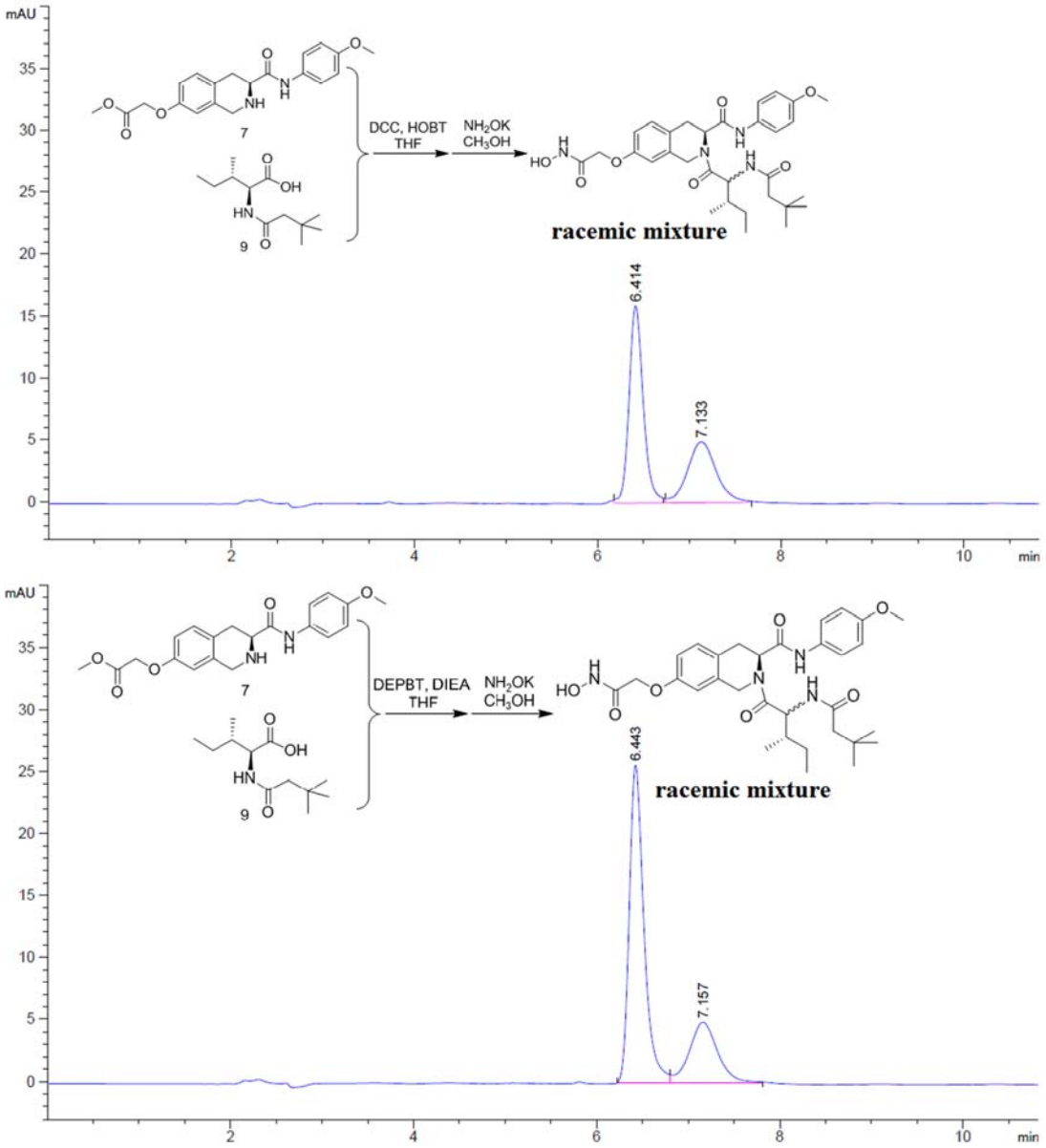

Fig. S7. Synthesis routes and HPLC chromatograms of racemic mixture of intermediate **10**

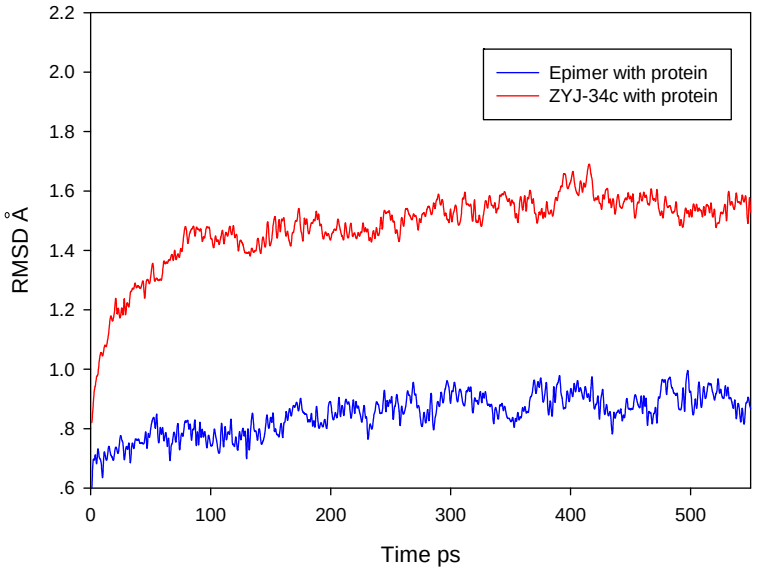

Fig. S8. RMSD plot of molecular dynamics simulations

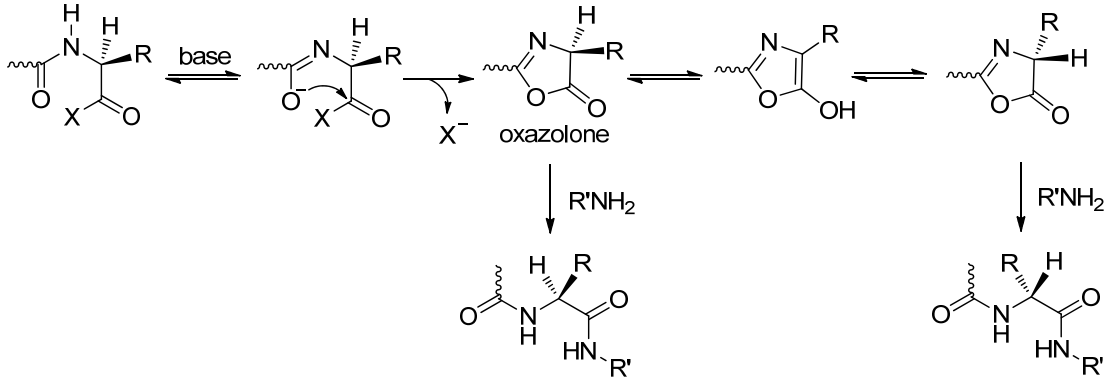

Scheme S1. Racemization mechanism involving oxazolone intermediate formation

Table S1. Contributions of the amino acid residues (PRO-23 and ASP-93) in the active site of HDAC2 to the binding free energy (kcal/mol).

Compd.	Amino acid residues	
	PRO-23	ASP-93
ZYJ-34c	-0.266	3.351
ZYJ-34c epimer	-0.769	-0.228

Experiment section

Chemistry. All commercially available starting materials, reagents and solvents were used without further purification. All reactions were monitored by TLC with 0.25 mm silica gel plates (60GF-254). UV light, iodine stain and ferric chloride were used to visualize the spots. Silica gel or C18 silica gel was used for column chromatography purification. ^{1}H NMR spectra were recorded on a Bruker DRX spectrometer at 600 MHz, δ in parts per million and *J* in hertz, using TMS as an internal standard. High-resolution mass spectra were conducted by Shandong Analysis and Test Center in Ji'nan, China. ESI-MS spectra were recorded on an API 4000 spectrometer. Melting points were determined uncorrected on an electrothermal melting point apparatus. HPLC analysis was performed on a Agilent 1100 HPLC instrument using a Phenomenex Synergi 4 μ Polar-RP 80A column (250 mm × 4.6 mm), eluted with 50% acetonitrile / 50% water (containing 0.1% formic acid), with detection at 254 nm and a flow rate of 1.0 mL/min.

Scheme 1

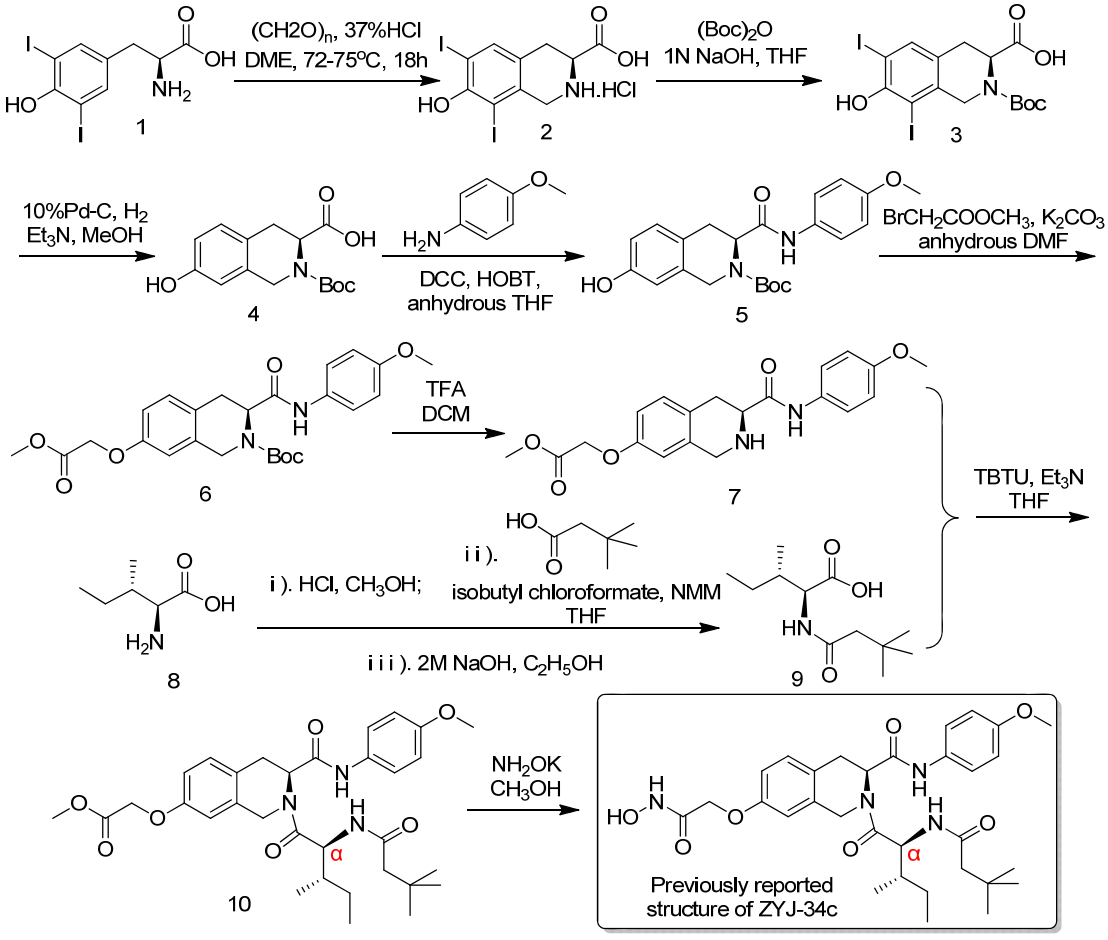

The reagents and conditions of Scheme 1 were reported in our previous work [1].

Scheme 2

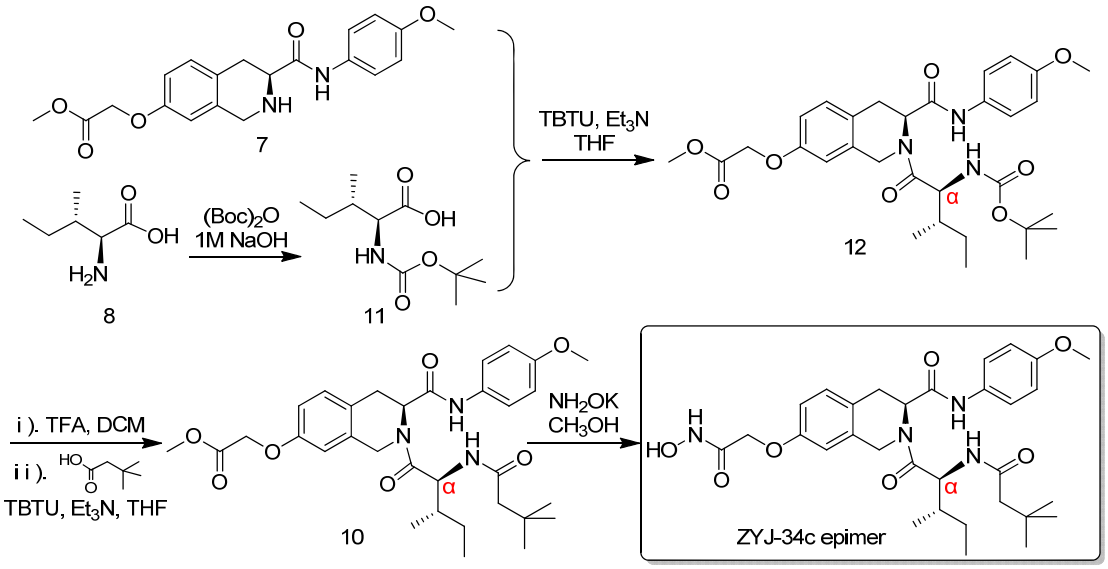

(2*S*,3*S*)-2-((*tert*-Butoxycarbonyl)amino)-3-methylpentanoic acid (11). To a solution of compound **8** (2.62 g, 20.0 mmol) in 44 mL of 1 N NaOH, was added a solution of $(Boc)_2O$ (4.80 g, 22.0 mmol) in THF (10 mL). The solution was kept between pH 9-11 by addition of 1 N NaOH. After stirring the mixture at room temperature for 8 h, THF was evaporated in vacuum with the residues being adjusted to pH 4-5 with 1 N aqueous citric acid. Then the mixture was extracted with EtOAc (3 × 25 mL). The extractions were combined, washed with brine (3 × 20 mL), dried over $MgSO_4$ and evaporated to give 4.39 g of crude product compound **11**. This product was used for the following reaction without further purification. ESI-MS *m/z*: 232.2 $[M+H]^+$.

Methyl 2-(((*S*)-2-((2*S*,3*S*)-2-((*tert*-butoxycarbonyl)amino)-3-methylpentanoyl)-3-((4-methoxyphenyl)carbamoyl)-1,2,3,4-tetrahydroisoquinolin-7-yl)oxy)acetate (12). At room temperature, to a solution of compound **11** (2.30 g, 10.0 mmol) in anhydrous THF (60 mL), was added Et_3N (1.12 g, 11.0 mmol) followed by 2-(1H-benzotriazole-1-yl)-1,1,3,3-tetramethyluronium tetrafluoroborate (TBTU, 3.56 g, 11.0 mmol). After 15 min, the amine compound **7** (3.70 g, 10.0 mmol) was added. Stirring was continued overnight, and then THF was evaporated with the residue being taken up in EtOAc (80 mL). The EtOAc solution was washed with saturated Na_2CO_3 (3 × 20 mL), 1 N HCl (3 × 20 mL), and brine (3 × 20 mL), dried over $MgSO_4$, and evaporated to give 4.68 g of crude product compound **12**. This product was used for the following reaction without further purification. ESI-MS *m/z*: 584.3 $[M+H]^+$.

Methyl 2-(((*S*)-2-((2*S*,3*S*)-2-(3,3-dimethylbutanamido)-3-methylpentanoyl)-3-((4-methoxyphenyl)carbamoyl)-1,2,3,4-tetrahydroisoquinolin-7-yl)oxy)acetate (10). To a solution of **12** (2.92 g, 5.0 mmol) in anhydrous dichloromethane (40 mL) was added

trifluoroacetic acid (12 mL). When the reaction was finished, Et_3N was added to the solution until the pH became weakly basic.

At room temperature, to a solution of 3,3-dimethylbutanoic acid (0.58 g, 5.0 mmol) in anhydrous THF (20 mL), was added Et_3N (0.56 g, 5.5 mmol) followed by 2-(1H-Benzotriazole-1-yl)-1,1,3,3-tetramethyluronium tetrafluoroborate (TBTU, 1.78 g, 5.5 mmol). After 15 min, aforementioned dichloromethane solution was added. Stirring was continued over night and then the solvent was evaporated with the residue being taken up in EtOAc (60 mL). The EtOAc solution was washed with 1 N HCl (3×15 mL), saturated Na_2CO_3 (3×15 mL) and brine (3×15 mL), dried over $MgSO_4$, and evaporated under vacuum. The crude product was purified by flash column chromatography (petroleum ether/EtOAc 2:1) to give 1.16 g of desired compound **10** as light yellow oil, which crystallized on standing, 39 % yield. ESI-MS *m/z*: 582.2 $[M+H]^+$.

(*S*)-2-((2*S*,3*S*)-2-(3,3-Dimethylbutanamido)-3-methylpentanoyl)-7-(2-(hydroxy amino)-2-oxoethoxy)-*N*-(4-methoxyphenyl)-1,2,3,4-tetrahydroisoquinoline-3-carb oxamide (ZYJ-34c epimer). To a solution of compound **10** (1.16 g, 2.0 mmol) in 20 mL of anhydrous methanol, was added a solution of NH_2OK (0.14 g, 6 mmol) in 3.5 mL of anhydrous methanol. The mixture was stirred for 0.5 h and the solvent was evaporated under vacuum. The residue was acidified with 2 N HCl until pH 5-6 then extracted with EtOAc (3×10 mL). The organic layers were combined, washed with brine (3×10 mL), dried over $MgSO_4$ and evaporated with the residue being purified by C18 reversed-phase column chromatography (H_2O/MeOH 3:7) to give 0.81 g of desired compound ZYJ-34c epimer as a white powder, 69 % yield. Mp: 130-132 °C. ^1H NMR and HRMS spectrums were shown in Figure S3 and Figure S4, respectively.

Scheme 3

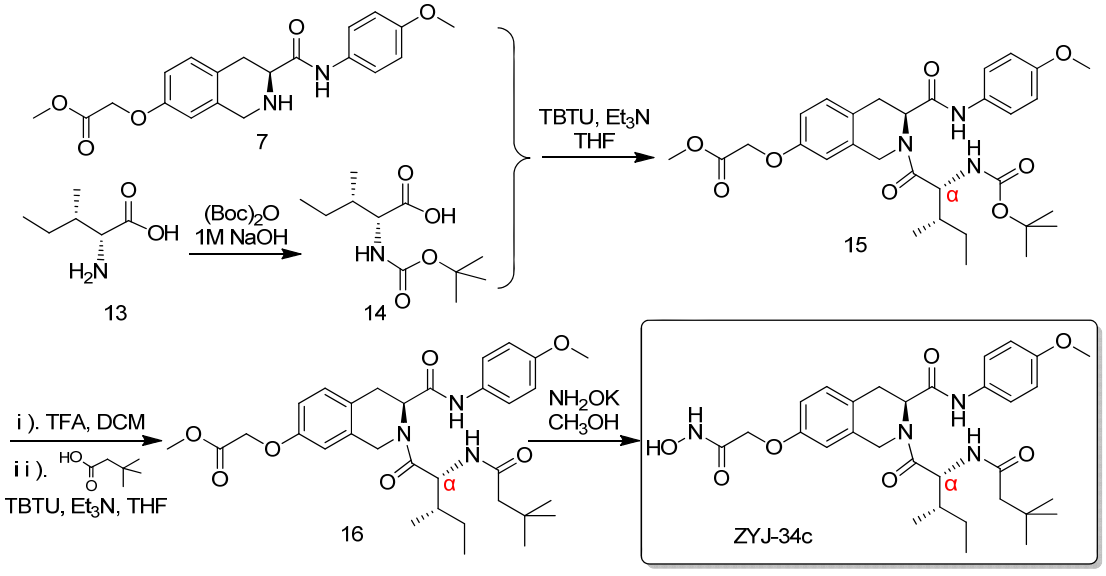

(2*R*,3*S*)-2-((*tert*-Butoxycarbonyl)amino)-3-methylpentanoic acid (14). Compound **14** was synthesized from **13** using the synthetic method for **11**. ESI-MS *m/z*: 232.2 $[M+H]^+$.

Methyl 2-(((*S*)-2-((2*R*,3*S*)-2-((*tert*-butoxycarbonyl)amino)-3-methylpentanoyl)-3-((4-methoxyphenyl)carbamoyl)-1,2,3,4-tetrahydroisoquinolin-7-yl)oxy)acetate (15). Compound **15** was synthesized from **14** and **7** using the synthetic method for **12**. ESI-MS *m/z*: 584.2 $[M+H]^+$.

Methyl 2-(((*S*)-2-((2*R*,3*S*)-2-(3,3-dimethylbutanamido)-3-methylpentanoyl)-3-((4-methoxyphenyl)carbamoyl)-1,2,3,4-tetrahydroisoquinolin-7-yl)oxy)acetate (16). Compound **16** was synthesized from **15** using the synthetic method for **10**. ESI-MS *m/z*: 582.2 $[M+H]^+$.

(*S*)-2-((2*R*,3*S*)-2-(3,3-Dimethylbutanamido)-3-methylpentanoyl)-7-(2-(hydroxyamino)-2-oxoethoxy)-*N*-(4-methoxyphenyl)-1,2,3,4-tetrahydroisoquinoline-3-carboxamide (ZYJ-34c). Using the synthetic method for ZYJ-34c epimer, compound **16** gave ZYJ-34c as a white powder. Mp: 123-125 °C. ^{1}H NMR and HRMS spectrums were shown in Figure S1 and Figure S2, respectively.

In Vitro HDACs Inhibition Fluorescence Assay. In vitro HDACs inhibition assays were conducted as previously described [1-3]. Boc-Lys (acetyl)-AMC substrate was used in inhibition assays against class I (HDAC1, HDAC2, HDAC3) and class IIb (HDAC6), while Boc-Lys (triflouroacetyl)-AMC substrate for class IIa (MDA-MB-231 cell lysate). In brief, 10 μL of enzyme solution was mixed with various concentrations of tested compound (50 μL). Five minutes later, fluorogenic substrate (40 μL) was added, and the mixture was incubated at 37 °C for 30 min and then stopped by addition of 100 μL of developer containing trypsin and TSA. After incubation at 37 °C for 20 min, fluorescence intensity was measured using a microplate reader at excitation and emission wavelengths of 390 nm and 460 nm, respectively. The inhibition ratios were calculated from the fluorescence intensity readings of tested wells relative to those of control wells, and the IC_{50} values were calculated using a regression analysis of the concentration/inhibition data.

In Vitro Antiproliferative Assay. In vitro antiproliferative assays were determined by the MTT (3-[4,5-dimethyl-2-thiazolyl]-2,5-diphenyl-2*H*-tetrazolium bromide) method as previously described [1-3]. Briefly, all cell lines were maintained in RPMI1640 medium containing 10% FBS at 37 ^oC in 5% CO_2 humidified incubator. Cells were passaged the day before dosing into a 96-well cell plate, allowed to grow for a minimum of 4 h prior to addition of compounds. After compounds addition, the plates were incubated for an additional 48 h, and then 0.5% MTT solution was added to each well. After further incubation for 4 h, formazan formed from MTT was

extracted by adding 200 μL of DMSO for 15 min. Absorbance was then determined using an ELISA reader at 570 nm and the IC_{50} values were calculated according to the inhibition ratios.

In Vivo Human Tumor Xenograft Models. In Vivo human tumor xenograft models were established as previously described [1-3]. In brief, tumor cell lines (MDA-MB-231) were cultured in RPMI1640 medium containing 10% FBS and maintained in a 5% CO_2 humidified incubator at 37 ^oC. For in vivo antitumor assays, aforementioned cells were inoculated subcutaneously in the right flanks of female athymic nude mice (BALB/c-nu, 5-6 weeks old, Slac Laboratory Aniamal, Shanghai, China). About ten days after injection, tumors were palpable (about 100 mm^3) and mice were randomized into treatment and control groups (5 mice per group). The treatment groups received 90 mg/kg of compounds by oral administration, and the blank control group received an equal volume of PBS solution containing DMSO. During treatment, subcutaneous tumors were measured with a vernier caliper every three days, and body weight was monitored regularly. After treatment, mice were sacrificed and dissected to weigh the tumor tissues and to examine the internal organ injury. Tumor growth inhibition (TGI) and relative increment ratio (T/C) were used as the evaluation indicators to reveal the antitumor effects in tumor weight and tumor volume, respectively. Data were analyzed by Student's two-tailed *t* test. A *P* level < 0.05 was considered statistically significant.

TGI = (the mean tumor weight of control group – the mean tumor weight of treated group) / the mean tumor weight of control group.

Tumor volumes (V) were estimated using the equation ($V = ab^2 / 2$, where a and b stand for the longest and shortest diameter, respectively). T/C was calculated according to the following formula:

T/C = the mean RTV of treated group / the mean RTV of control group.

RTV, namely relative tumor volume = V_t / V_0 (V_t: the tumor volume measured at the end of treatment; V_0: the tumor volume measured at the beginning of treatment).

Molecular Modeling. Before carrying out molecular dynamics simulation, compounds ZYJ-34c and its epimer were minimized and docked into binding site of the crystal structure of HDAC2 (PDB ID: 3MAX) by Surflex-Dock module [4] in Sybyl-X1.1. Then the partial charges of inhibitors were determined by RESP method [5] and the General Amber force field [6] was assigned to the inhibitors. The standard Amber ff10 force field [7] was used to parameter the protein. The Stote non-bounded model was used for Zn^{2+} as it was proved to be the most efficient when compared with other method [8]. The tleap module in AmberTools was used to generate the initial coordinate and topology files. The complexes were put into a TIP3P water box [9] containing appropriate amount of Na^+ ions, respectively. Then the sander module

of Amber11 was used to perform molecular dynamics (MD) simulations. Systems were minimized by 2000 steps of steepest descent and 2000 steps of conjugated gradients. Then the systems were heated from 0 K to 300 K for 50 ps and equilibrated at 300 K for 50 ps. Finally the two systems were run for a 450 ps production, respectively. After MD simulation, the MM-GBSA method [10, 11] was used to calculate the Gibbs free energy.

References

1. Zhang, Y.; Fang, H.; Feng, J.; Jia, Y.; Wang, X.; Xu, W. Discovery of a Tetrahydroisoquinoline-Based Hydroxamic Acid Derivative (ZYJ-34c) as Histone Deacetylase Inhibitor with Potent Oral Antitumor Activities. *J. Med. Chem.*, **2011**, *54*, 5532-5539.
2. Zhang, Y.; Feng, J.; Jia, Y.; Wang, X.; Zhang, L.; Liu, C.; Fang, H.; Xu, W. Development of tetrahydroisoquinoline-based hydroxamic acid serivatives: potent histone deacetylase inhibitors with marked in vitro and in vivo antitumor activities. *J. Med. Chem.*, **2011**, *54*, 2823-2838.
3. Zhang, Y.; Yang, P.; Chou, C. J.; Liu, C.; Wang, X.; Xu, W. Development of N-Hydroxycinnamamide-Based Histone Deacetylase Inhibitors with an Indole-Containing Cap Group. *ACS Med. Chem. Lett.*, **2013**, *4*, 235-238.
4. Jain, A. N. Surflex-Dock 2.1: robust performance from ligand energetic modeling, ring flexibility, and knowledge-based search. *J. Comput. Aided Mol. Des.*, **2007**, *21*, 281-306.
5. Bayly, C. I.; Cieplak, P.; Cornell, W.; Kollman, P. A. A well-behaved electrostatic potential based method using charge restraints for deriving atomic charges: the RESP model. *J. Phys. Chem.*, **1993**, *97*, 10269-10280.
6. Wang, J., Wolf, R. M.; Caldwell, J. W.; Kollman, P. A.; Case, D. A. Development and testing of a general amber force field. *J. Comput. Chem.*, **2004**, *25*, 1157-1174.
7. Cornell, W. D., Cieplak, P.; Bayly, C. I.; Gould, I. R.; Merz, K. M.; Ferguson, D. M.; Spellmeyer, D. C.; Fox, T.; Caldwell, J. W.; Kollman, P. A. A second generation force field for the simulation of proteins, nucleic acids, and organic molecules. *J. Am. Chem. Soc.*, **1995**, *117*, 5179-5197.
8. Stote, R. H.; Karplus, M. Zinc Binding in Proteins and Solution: A Simple but Accurate Nonbonded Representation. *Proteins*, **1995**, *23*, 12-31.
9. Jorgensen, W. L.; Chandrasekhar, J.; Madura, J. D.; Impey, R. W.; Klein, M. L. Comparison of simple potential functions for simulating liquid water. *J. Chem. Phys.*, **1983**, *79*, 926-936.

10. Donini, O. A.; Kollman, P. A. Calculation and prediction of binding free energies for the matrix metalloproteinases. *J. Med. Chem.*, **2000**, *43*, 4180-4188.

11. Huang, D.; Li, X.; Wei, Y.; Xiu, Z. A novel series of L-2-benzyloxycarbonylamino-8-(2-pyridyl)-disulfidyloctanoic acid derivatives as histone deacetylase inhibitors: design, synthesis and molecular modeling study. *Eur. J. Med. Chem.*, **2012**, *52*, 112-122.